

2

AD-A247 619



Space Division Switches Based on Semiconductor Optical Amplifiers

1991

R. F. Kalman, L. G. Kazovsky, and J. W. Goodman

Department of Electrical Engineering

Stanford University, Stanford, CA 94305

N00014-91-5-1857

Abstract

Semiconductor optical amplifiers (SOAs) can be used in space-division (SD) switches to provide both switching and optical gain. We present a general analysis of optical switches using SOAs, considering noise and saturation effects associated with amplified spontaneous emission. Based on this analysis, we derive size limitations of SD switches.

Three specific SD switching architectures are considered. For a the lumped gain matrix-vector multiplier (MVM) switch, switch sizes are limited to the range of 3000x3000 for SOAs with saturation output powers of 100 mW. Based on the effects considered in our analysis, distributed gain MVM switches and Benes switches are not limited by signal-to-noise ratio and saturation up to sizes of $10^{80} \times 10^{80}$ for SOAs with saturation output powers of 100 mW.



This document has been approved for public release and sale; its distribution is unlimited.

92 2 28 064

92-05224



1. Introduction

To overcome the bottleneck imposed by the node electronics in time-division multiplexed systems, space-division (SD) switching techniques can be used. In all-optical SD switches, traffic is routed between nodes on spatially distinct channels without opto-electronic conversion between the source and destination nodes.

All-optical switches can be constructed using optical splitters, combiners, and binary on/off optical switches, each of which has optical loss. Optical amplifiers can be used to overcome these losses [1]. In SD switches, semiconductor optical amplifiers (SOAs) have the advantage over erbium-doped fiber amplifiers that they can be switched quickly, are smaller, and are amenable to monolithic integration with passive waveguiding structures and electronics.

The objective of this paper is to evaluate the limitations on the number of inputs and outputs (the switch "size") for all-optical SD switches which utilize SOAs as both switching elements and amplifiers, based on signal-to-noise ratio and saturation constraints. In Section 2, we analyze the behavior of SOAs and the behavior of systems based on SOAs. In Section 3, we evaluate the size limitations of three specific switch implementations. Discussion and conclusions are presented in Sections 4 and 5, respectively.

2. SOA and Switch Behavior

2.1 The Evolution of Spontaneous Emission

The optical power at the output of a SOA, P_{out} , is related to the input power, P_{in} , by

$$P_{out} = L_{in}L_{out}GP_{in} + L_{out}pn_{sp}(G-1)h\nu_c\Delta\nu, \quad (1)$$

where G is the internal SOA gain, L_{in} and L_{out} are the input and output coupling losses to the SOA, respectively, ν_c is the center frequency of the amplifier bandpass, and $\Delta\nu$ is the effective amplifier bandwidth. n_{sp} is the excess spontaneous emission factor [2] and p is a factor which ranges from 1 for a device which amplifies only one polarization to 2 for a polarization-insensitive device.

Statement A per telecon
Dr. Rabinder Madan ONR/Code 1114
Arlington, VA 22217-5000

NWW 3/16/92

Dist:	Approved for Release
A-1	

Consider a system with M identical “stages,” each stage consisting of a system loss, L_s , and a SOA with its associated coupling losses. Using Eq. (1), we find that the power output from the M^{th} stage, P_M , is given by

$$P_M = G_{sig} P_{in} + G_{sp} n_{sp} p_{eff} h \nu_c \Delta \nu_{eff} \quad (2)$$

where $\Delta \nu_{eff}$ is the effective overall gain bandwidth and p_{eff} is the effective p which ranges from 1 to 2. The net signal gain, G_{sig} , and the net spontaneous “gain”, G_{sp} , are given by

$$G_{sig} = (L_s L_{in} L_{out} G)^M \quad (3)$$

$$G_{sp} = (G - 1) L_{out} \frac{1 - G_{sig}}{1 - G_{sig}^{1/M}} \cong M(G - 1) L_{out} \frac{G_{sig} - 1}{\ln G_{sig}} \quad (4)$$

The second equality in Eq. (4) holds for large M .

2.2 Saturation and Signal-to-Noise Ratio Constraints

Due to the high spontaneous emission and signal levels emerging from a SOA-based switching system, the post-detection noise is typically dominated by signal-spontaneous and spontaneous-spontaneous beat noise. This leads to a post-detection signal-to-noise ratio (SNR), γ , of approximately [3]

$$\gamma = \frac{(G_{sig} P_{in})^2}{4 G_{sp} n_{sp} h \nu_c B_e (G_{sig} P_{in} + G_{sp} n_{sp} h \nu_c B_o)} \quad (5)$$

where B_e is the electrical noise bandwidth of the receiver and B_o ($B_o < \Delta \nu_{eff}$) is the bandwidth of an optical filter placed in front of the receiver. To achieve a 10^{-9} bit error ratio (BER), we require $\gamma > 144$.

SOAs exhibit nonlinear distortion due to gain saturation which is characterized by a saturation output power, P_{sat} , at which the gain has dropped to $1/e$ of its unsaturated value [4]. Saturation leads to a number of undesirable effects effects: a decrease in gain, intersymbol interference (ISI) and, in frequency-division multiplexed systems, crosstalk. We consider the simple saturation constraint

$$\left(G_{sig} P_{in} + G_{sp} P_{eff} n_{sp} h \nu_c \Delta \nu_{eff} \right) \frac{1}{L_{out}} \leq P_{sat} \quad (6)$$

Eq. 9 indicates that the total power emerging from the endface of the last SOA in the cascaded amplifier system (i.e. before its output coupling loss) must be less than P_{sat} .

2.3 Specific Switching Architectures

In this paper, we examine two versions of the matrix-vector multiplier (MVM) crossbar switch (Fig. 1) and the Benes switch (Fig. 2). The regular structure of the three switches allows the direct application of the analysis of Section 2.1. The number of SOAs, the number of stages, and the system loss per stage (L_s) are given in Table 1 for the three switches.

The MVM architectures allow completely general interconnections between the inputs and outputs. Switching occurs only in the “switching plane” in the center of the switch. In the lumped gain MVM (LGMVM) switch, SOAs are placed only in the switching plane and at the output. In the distributed gain MVM (DGMVM) switch, SOAs are placed after each 1x2 splitter and 2x1 combiner. In the Benes switch, 2x2 switches arranged in switching “planes” provide a rearrangeably nonblocking interconnection [1].

3. System Size Limitations

We consider system size limitations based on two phenomena: required signal-to-noise ratio (SNR) at the system output, and saturation of the SOAs. For a given value of the signal gain, G_{sig} , we can solve Eqs. (5) and (6) simultaneously to find the maximum allowable spontaneous gain, $G_{sp max}$, and the optimum input signal level. Using this result and solving Eq. (4) for the maximum permissible number of stages, M_{max} , we find

$$M_{max} = \frac{G_{sp max}}{(G - 1)L_{out}} \frac{\ln G_{sig}}{G_{sig} - 1} \quad (7)$$

Recalling the relationship between M and N for a distributed gain MVM switch (see Table 1), we find

$$N_{max} = 2^{\frac{G_{sp\ max}}{2(G-1)L_{out}} \frac{\ln G_{sig}}{G_{sig}-1}} \quad (8)$$

For the Benes switch, we find that N_{max} is a factor of $\sqrt{2}$ larger than for the DGMVM switch. A plot of N_{max} vs. P_{sat} is shown in Fig. 3 for a DGMVM switch. The curves are virtually identical for the Benes switch.

For the LGMVM switch, from Table 1 we see that $M = 2$ and $L_s = 1/N$. We can solve for G as a function of N in Eq. (3) and substitute this in Eq. (4) to find

$$N_{max} = \frac{L_{in} G_{sp\ max}}{2\sqrt{G_{sig}}} \frac{\ln G_{sig}}{G_{sig}-1} + \frac{L_{in} L_{out}}{\sqrt{G_{sig}}} \quad (9)$$

A plot of N_{max} vs. P_{sat} is shown in Fig. 4 for a LGMVM switch.

4. Discussion

Current devices exhibit saturation power levels (P_{sat}) in the range of 1 - 100 mW (the latter being achieved in quantum well devices). Fig. 3 indicates that when gain is distributed throughout the switching fabric and SOAs with $P_{sat} = 100$ mW, SNR and saturation considerations do not limit switch the switch size up to approximately $10^{80} \times 10^{80}$. By contrast, lumped gain systems such as the LGMVM switch are limited to sizes of less than 3000×3000 for all values of P_{sat} . The impact of pre-detection optical filtering on maximum switch size is noticeable, but not nearly as significant as the effect of increasing P_{sat} .

Though the very large switch sizes predicted above may seem to have little meaning, the equivalent of signal path through a very large switch can easily be obtained by cascading smaller switches (this can be seen by considering the relationships between N and M in Table 1). A path equivalent to that through a $10^{80} \times 10^{80}$ DGMVM switch is encountered traversing 80 cascaded 10×10 switches or 40 cascaded 100×100 switches.

Crosstalk may play a role in distributed gain SD switching systems, which utilize low gain devices. Crosstalk results from the nonzero transmission of SOAs in the off state (no applied current). At the expense of increasing α_{sp} , the off-state absorption of an SOA can

be made arbitrarily large by increasing its length. Fig. 3 assumes a n_{sp} of 5, which corresponds to an off-state absorption of 40 dB for a device with an internal gain of 10. This high absorption prevents crosstalk from impacting system performance.

5. Conclusions

Semiconductor optical amplifiers (SOAs) may play a useful role in optical space-division (SD) switching systems, since they provide both optical gain and fast switching. The sizes of optical switches based on SOAs are ultimately limited by signal-to-noise ratio (SNR) and saturation considerations, both of which are associated with spontaneous emission from the SOAs.

In distributed gain matrix-vector multiplier (MVM) and Benes switches, gain is distributed throughout the switching fabric. By utilizing SOAs with $P_{sat} = 100$ mW, SNR and saturation considerations do not limit the size of these distributed gain switches up to approximately $10^{80} \times 10^{80}$. By contrast, lumped gain switches such as the lumped gain MVM switch are limited in size to less than 3000×3000 for $P_{sat} = 100$ mW. Because the complexity of Benes switches is of order $N \log N$ vs. N^2 for MVM switches, Benes-like switches may be preferred for implementing large switching systems.

Acknowledgement

This work was partially supported by ONR contract #N00014-91-J-1857.

References

- [1] J. D. Evankow and R. A. Thompson, "Photonic Switching Modules Designed with Laser Diode Amplifiers," *IEEE J. Select. Areas Commun.*, vol. 6, pp. 1087-1094, 1988.
- [2] C. H. Henry, "Theory of Spontaneous Emission Noise in Open Resonators and its Application to Lasers and Optical Amplifiers," *J. Lightwave Technol.*, vol. 4, no. 3, pp. 288-297, 1986.
- [3] N. A. Olsson, "Lightwave Systems with Optical Amplifiers," *J. Lightwave Technol.*, vol. 7, no. 7, pp. 1071-1082, 1989.
- [4] A. A. M. Saleh and I. M. I. Habbab, "Effects of Semiconductor-Optical-Amplifier Nonlinearity on the Performance of High-Speed Intensity-Modulation Lightwave Systems," *IEEE Trans. Commun.*, vol. 38, no. 6, pp. 839-846, 1990.

Figure Captions

Table 1. Number of SOAs, number of stages (M), and system loss per stage (L_s), for LGMVM, DGMVM, and Benes switches of size N .

Figure 1. MVM crossbar switches: (a) lumped gain; (b) distributed gain. As an example, 4x4 switches are shown.

Figure 2. Benes switch. As an example, a 4x4 switch is shown

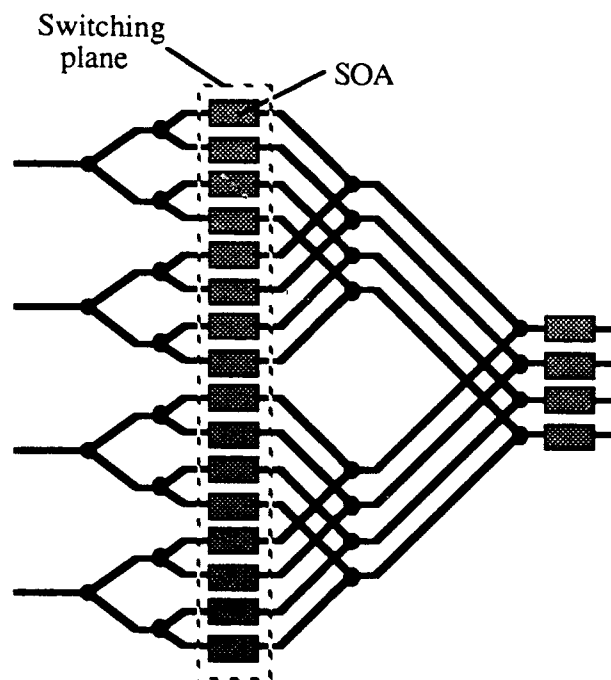
Figure 3. Maximum switch size vs. P_{sat} for the DGMVM switch.

Figure 4. Maximum switch size vs. P_{sat} for the LGMVM switch.

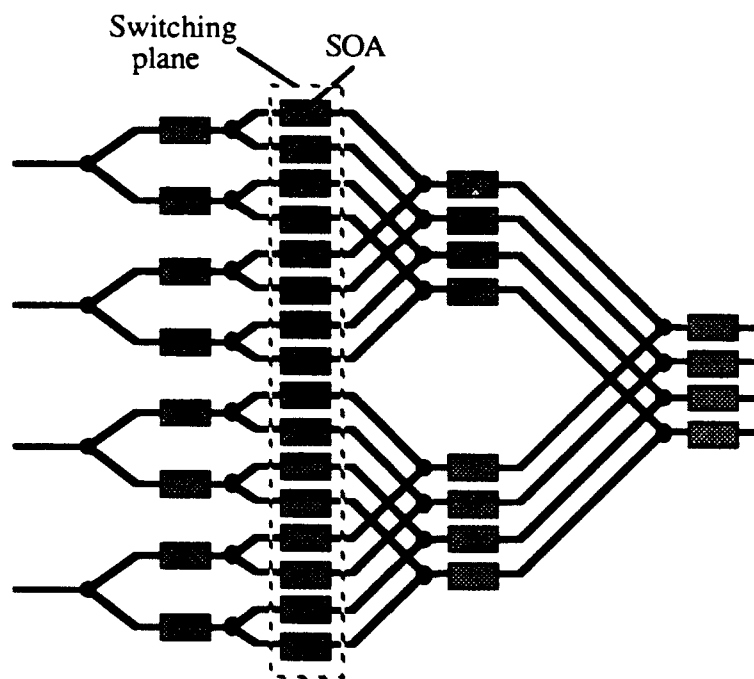
Table 1

	LGMVM	DGMVM	Benes
Number of SOAs	$N(N+1)$	$N(3N-2)$	$4N(\log_2 N - 0.5)$
Number of stages	2	$2 \log_2 N$	$2 \log_2 N - 1$
System Loss per Stage	$1/N$	0.5	0.5

Figure 1



(a)



(b)

Figure 2

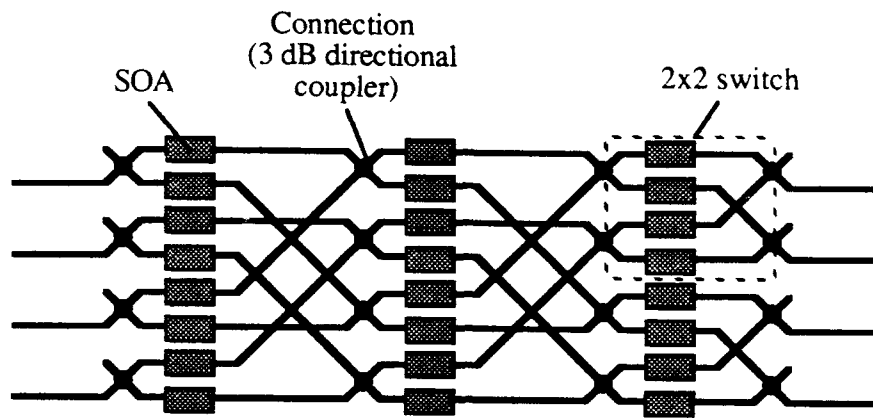


Figure 3

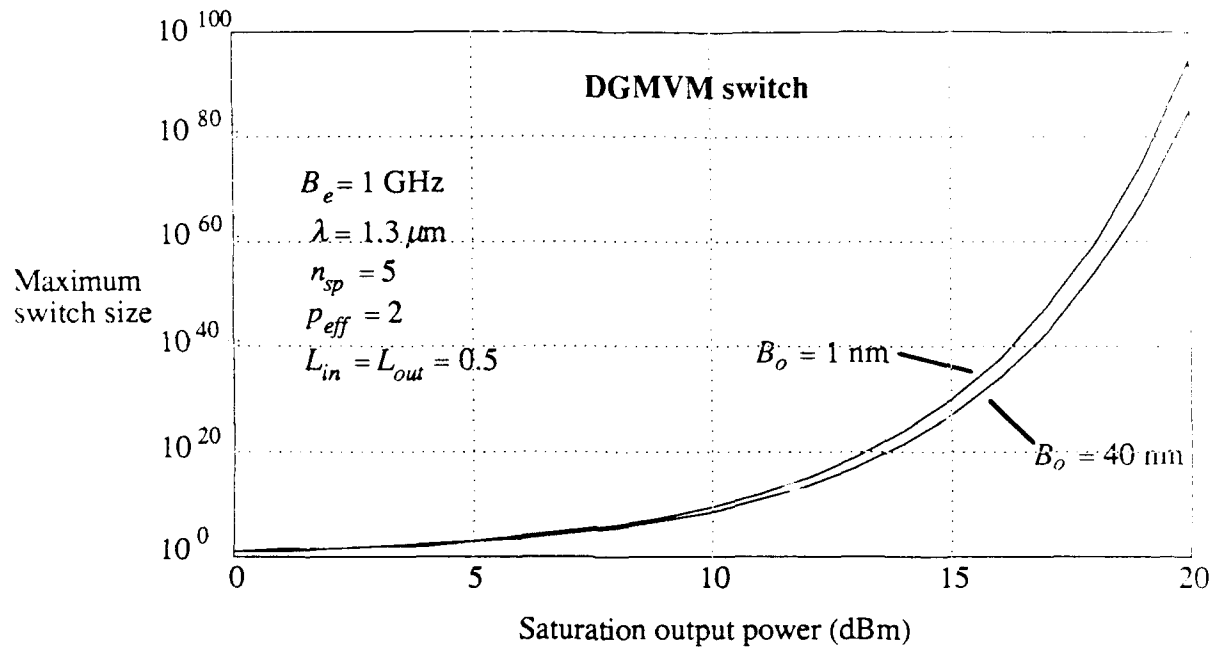


Figure 4

